



Article

Recent Activity and Kinematics of the Bounding Faults of the Catanzaro Trough (Central Calabria, Italy): New Morphotectonic, Geodetic and Seismological Data

Claudia Pirrotta ¹, Graziella Barberi ², Giovanni Barreca ^{1,3} , Fabio Brighenti ¹, Francesco Carnemolla ¹ ,
Giorgio De Guidi ^{1,3}, Carmelo Monaco ^{1,2,3,*} , Fabrizio Pepe ⁴  and Luciano Scarfi ²

¹ Dipartimento di Scienze Biologiche Geologiche e Ambientali, Università di Catania, 95129 Catania, Italy; claudiapirrotta@hotmail.com (C.P.); g.barreca@unict.it (G.B.); fabio.brighenti@phd.unict.it (F.B.); francesco.carnemolla@unict.it (F.C.); deguidi@unict.it (G.D.G.)

² Istituto Nazionale di Geofisica e Vulcanologia, Osservatorio Etneo—Sezione di Catania, 95125 Catania, Italy; graziella.barberi@ingv.it (G.B.); luciano.scarfi@ingv.it (L.S.)

³ CRUST—Interuniversity Center for 3D Seismotectonics with Territorial Applications, 66100 Chieti, Italy

⁴ Dipartimento di Scienze della Terra e del Mare, Università di Palermo, 90123 Palermo, Italy; fabrizio.pepe@unipa.it

* Correspondence: cmonaco@unict.it; Tel.: +39-095-7195-731



Citation: Pirrotta, C.; Barberi, G.; Barreca, G.; Brighenti, F.; Carnemolla, F.; De Guidi, G.; Monaco, C.; Pepe, F.; Scarfi, L. Recent Activity and Kinematics of the Bounding Faults of the Catanzaro Trough (Central Calabria, Italy): New Morphotectonic, Geodetic and Seismological Data. *Geosciences* **2021**, *11*, 405. <https://doi.org/10.3390/geosciences11100405>

Academic Editors:
Ioannis Koukouvelas,
Riccardo Caputo, Tejpal Singh and
Jesus Martinez-Frias

Received: 3 September 2021
Accepted: 23 September 2021
Published: 26 September 2021

Publisher's Note: MDPI stays neutral with regard to jurisdictional claims in published maps and institutional affiliations.



Copyright: © 2021 by the authors. Licensee MDPI, Basel, Switzerland. This article is an open access article distributed under the terms and conditions of the Creative Commons Attribution (CC BY) license (<https://creativecommons.org/licenses/by/4.0/>).

Abstract: A multidisciplinary work integrating structural, geodetic and seismological data was performed in the Catanzaro Trough (central Calabria, Italy) to define the seismotectonic setting of this area. The Catanzaro Trough is a structural depression transversal to the Calabrian Arc, lying in-between two longitudinal grabens: the Crati Basin to the north and the Mesima Basin to the south. The investigated area experienced some of the strongest historical earthquakes of Italy, whose seismogenic sources are still not well defined. We investigated and mapped the major WSW–ENE to WNW–ESE trending normal-oblique Lamezia-Catanzaro Fault System, bounding to the north the Catanzaro Trough. Morphotectonic data reveal that some fault segments have recently been reactivated since they have displaced upper Pleistocene deposits showing typical geomorphic features associated with active normal fault scarps such as triangular and trapezoidal facets, and displaced alluvial fans. The analysis of instrumental seismicity indicates that some clusters of earthquakes have nucleated on the Lamezia-Catanzaro Fault System. In addition, focal mechanisms indicate the prevalence of left-lateral kinematics on E–W roughly oriented fault plains. GPS data confirm that slow left-lateral motion occurs along this fault system. Minor north-dipping normal faults were also mapped in the southern side of the Catanzaro Trough. They show eroded fault scarps along which weak seismic activity and negligible geodetic motion occur. Our study highlights that the Catanzaro Trough is a polyphased Plio-Quaternary extensional basin developed early as a half-graben in the frame of the tear-faulting occurring at the northern edge of the subducting Ionian slab. In this context, the strike-slip motion contributes to the longitudinal segmentation of the Calabrian Arc. In addition, the high number of seismic events evidenced by the instrumental seismicity, the macroseismic intensity distribution of the historical earthquakes and the scaling laws relating to earthquakes and seismogenic faults support the hypothesis that the Lamezia-Catanzaro Fault System may have been responsible for the historical earthquakes since it is capable of triggering earthquakes with magnitude up to 6.9.

Keywords: Calabrian Arc; morphotectonics; geodetic data; instrumental seismicity

1. Introduction

The Calabrian Arc (CA hereafter) is an arc-shaped sector of the Apennine-Maghrebian chain structured in the frame of the NW convergence between Eurasia and the Nubia plates [1] (Figure 1A). Since the middle Miocene, this region has been affected by extensional

and strike-slip tectonics, superimposed on the pre-existing collisional context [2]. Since the Late Neogene period, part of the European margin was extruded SE-wards with respect to the adjacent collisional sectors to form the CA [3,4]. Tensional strain, localised in the central-internal sectors of the arc and responsible for the development of longitudinal graben with respect to the orogenic front (e.g., Crati, Mesima, Messina Strait), can be ascribed to the southeastward rollback of the Ionian subducting slab [5–7].

Despite numerous tectonic, seismological and geodetic studies, the Plio-Quaternary evolution of the CA is still a matter of debate due to the high structural complexity of the region. In particular, the origin and geodynamic link between the transversal structures (including the Catanzaro Trough), characterised by a strike-slip component of motion, and the longitudinal extensional basins, is still unclear (e.g., [8]). Whatever the evolutionary model, both longitudinal and transversal faults are considered the source of the most destructive historical earthquakes of the Italian regions [9,10]. Consequently, the CA is characterised by the largest concentration of seismic moment release [11–14] and the highest probability of the occurrence of major earthquakes [15]. As regards the Catanzaro Trough, macroseismic data suggest that the last destructive event of the 1783 seismic sequence, which hit all southern Calabria from February 5 to March 28 (maximum Magnitude $M_w \sim 7.03$; $I_0 \sim XI$ MCS [16]), was located in this area. However, the epicentral location of this shock and other earthquakes that occurred in the same area is still debated.

This work aims to clarify the geometry, kinematics and activity of the faults bounding the Catanzaro Trough to define their seismogenic potential. In this frame, we used a multidisciplinary study consisting of (i) morphotectonic study through DEM, Lidar rendering and aerial stereopairs to map tectonic features; (ii) qualitative geomorphological investigations to highlight possible recent fault activity; (iii) geological structural surveys carried out on the most relevant faults to define their recent kinematics; (iv) analysis of seismological and geodetic data.

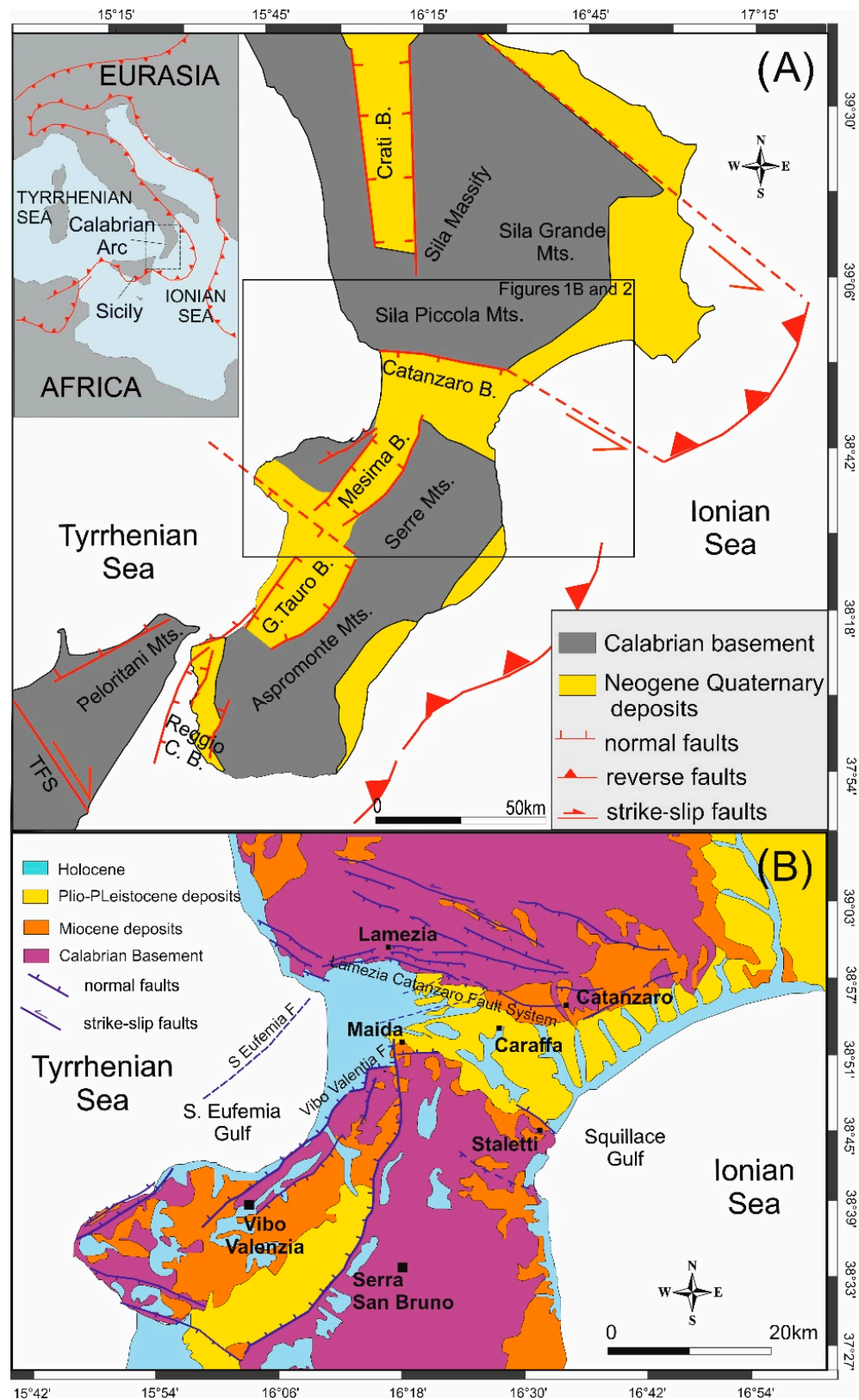


Figure 1. (A) Simplified geological map of the Calabrian Arc with the main structural elements from Van Dijk et al. [17] and Ghisetti [18,19]; TFS is the Tindari Fault System. Inset shows the Alpine-Apenninic-Maghrebian orogen in the context of the Eurasia-Nubia convergence; (B) Geological sketch map of the Central Calabria.

2. Geodynamic and Geological Setting

2.1. The Calabrian Arc

The northwestward subduction of the Ionian lithosphere below the CA was responsible for developing a complex back-arc/forearc/trench system [1]. The presence of distinct lithospheric domains, such as the continental crust of the Pelagian Block (Nubia Plate) and the Apulian Block (Adria Plate), and the oceanic crust of the Ionian Basin between them, has strongly influenced the geodynamic evolution of the subduction system. Due to these crustal heterogeneities, the plates convergence caused (i) diachronous collisional processes at the northern and southern boundaries of the CA [17], where the Apenninic-Maghrebian chain built up, (ii) the formation of an accretionary wedge in the Ionian Sea [20] and (iii) the opening of the back-arc in the Tyrrhenian Basin [21]. Subduction migrated eastward from the Tortonian to Early Pliocene and southeastward from the Late Pliocene to Early Pleistocene [3,4,21,22]. Currently, the subduction of the oceanic crust continues only in a narrow sector between the Tindari Fault System to the south and the Catanzaro Trough to the north [23–26] (Figure 1A). The southwestern edge of the slab is represented by a NW–SE trending structure classified as a Subduction-Transform Edge Propagator (STEP) highlighted by an abrupt ending of the deep seismicity [25–27]. In the northeastern sector, the subduction terminates with a lateral ramp marking the transition from subduction in the CA to collision in the Southern Apennines [24,28].

Instrumental seismicity (Figure 2A) confirms the occurrence of a slab window at depths between 100 and 200 km beneath the Catanzaro Trough [23–27]. Recently, Maesano et al. [24] hypothesised the presence of an incipient longitudinal slab tear in the deeper part of the slab (below 20 km) with progressively increasing offset from south to north and interpreted this tear as the ongoing southward propagation of the slab window.

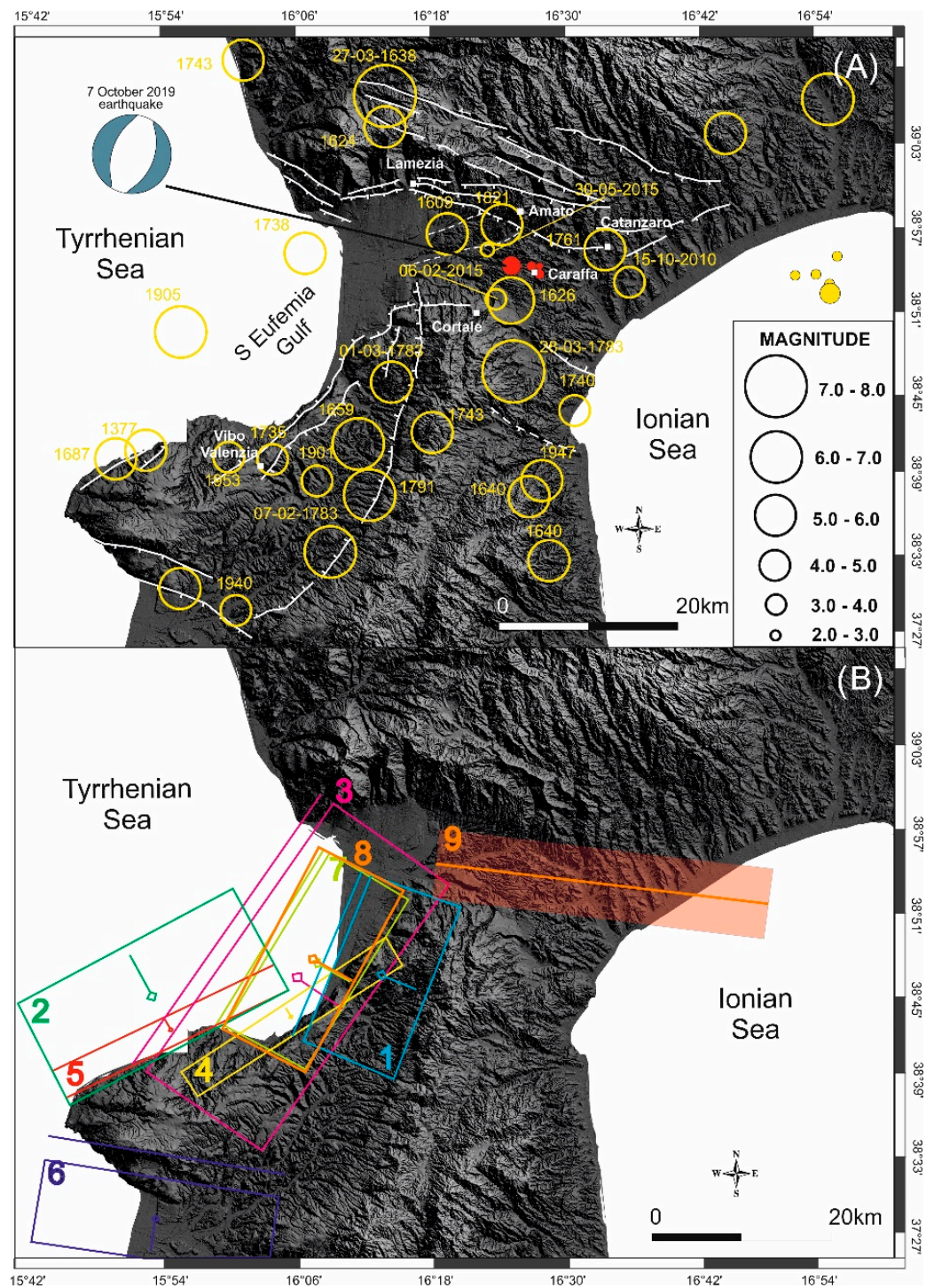


Figure 2. (A) Historical and instrumental seismicity of the investigated area (see Figure 1A for location), with magnitude higher than 4.8 (CPTI, [16]); the 2017 and 2019 seismic sequence are reported though they have magnitude lower than 4.8: filled yellow circles are the seismic sequence that occurred in July 2017; filled red circles are the seismic sequence of October 2019; focal solution refers to the 7 October 2019 earthquake; white lines with barbs are normal faults, white lines with arrows are strike slip faults; (B) Seismogenic sources of the 1905 earthquake from the literature (see also [29]): (1) Angitola Fault [30]; (2) Capo Vaticano Fault [10]; (3) Angitola Fault [31]; (4) Vibo Valentia Fault [32]; (5) Capo Vaticano Fault [32]; (6) Coccorino Fault [33,34]; (7) Santa Eufemia Fault [29], (8) Santa Eufemia Individual Seismogenic Source [35]; (9) Caraffa-Squillace Gulf composite seismogenic source [35].

In the upper crustal sector, the evolution of the CA is controversial. According to Ghisetti and Vezzani [8], the opening of longitudinal grabens and fan-like transverse troughs can be genetically related to the progressive thickening and bowing, respectively, of the CA since the Neogene phase of its SE-ward migration. According to Van Dijk et al. [17], since the Miocene epoch, five major transpressive crustal shear zones, which root into many deep thick-skinned overthrusts, have dissected and deformed the Early Miocene thrust sheet pile. These fault systems caused the structuration of highs and longitudinal and transversal sedimentary basins such as the Catanzaro Trough (see also [2]). Other authors [36–38] suggest that these basins developed as a consequence of strike-slip and transtensional tectonics related to different advancements of distinct sectors of the CA. From the middle Pleistocene, contraction was replaced by orogenic extension, which also caused the development of N–S to NE–SW trending normal faults that diffusely offset late Quaternary deposits [2,9,10,39].

From the middle Pleistocene, a fast regional uplift (~1 mm/yr), likely due to asthenosphere flow or wedging (e.g., [27,40,41]), contributed to the development of Pleistocene marine terraces and Holocene paleo-shorelines, the former reaching altitudes of 1200 m a.s.l., mainly along the western Calabria coastline [19,42–46].

2.2. The Catanzaro Trough

The Catanzaro Basin is filled by Pliocene–Quaternary sedimentary sequences, consisting of marine and continental deposits, unconformably lying on the CA structural units [47–49] (Figure 1B). The CA units encompass Hercynian metamorphic and magmatic rocks, Mesozoic carbonate platform, and middle–late Miocene terrigenous sequences ([17] and reference therein). The thickness of Pleistocene deposits in the Catanzaro Trough is higher in the northwestern sector. Here, large and widespread alluvial fans [39], likely due to the activity of prevalently normal faults (Figure 1B) occur. The southern border of the Catanzaro Trough is characterised by on-lapping of Pliocene–Quaternary deposits on crystalline nappes. The top of the sedimentary succession is represented by middle–upper Pleistocene marine terraces made up of siliciclastic sands and sandstones, with poor fossiliferous content [39].

The development of the Catanzaro Trough has been controlled by the activity of a primary WNW–ESE to WSW–ENE trending fault system (Figure 1B), the Lamezia–Catanzaro Fault System, which bound the basin to the north. Two minor north-dipping faults, the Maida Fault and the Staletti Fault bound the basin to the south [2,39]. The Lamezia–Catanzaro Fault System shows a clear morphologic expression and structural continuity. It is composed of distinct normal/oblique-slip faults, locally arranged in a left-stepping en-echelon pattern (see also [2]). The Lamezia–Catanzaro Fault System shows significant evidence of recent normal faulting in the western sector, where Punzo et al. [50] have recently demonstrated that it is still active but hidden by Holocene deposits. According to Brutto et al. [39], during the late Miocene–early Pliocene, the WNW–ESE trending fault systems were characterised by left-lateral kinematics, switching to right-lateral during the late Pliocene and to extensional kinematics since the middle Pleistocene. This extension, WNW–ESE oriented (see also [10]), has also been accommodated by NE–SW and, subordinately, N–S oriented normal faults producing horst and graben association in the Catanzaro Trough, affecting late Quaternary deposits. Recently, Corradino et al. [51] found evidence of recent activity along NE–SW trending faults in the Sant’Eufemia Gulf that allowed to infer the occurrence of an active ~E–W oriented left-lateral transtensional shear zone, extending as far as the Squillace Gulf (Ionian offshore). According to the authors, this likely represents the upper plate response to a tear fault of the lower plate (see also [52]).

The historical and instrumental seismicity testifies to the present-day high tectonic activity of the Catanzaro Trough. This area was the place of several historical earthquakes (Figure 2A), such as the 1609 ($M_w = 5.8$, $I_o = VIII$ – IX [16]), the 1626 ($M_w = 6.07$, $I_o = IX$ [16]), the 1761 ($M_w = 5.10$, $I_o = VII$ [16]) and the 1821 ($M_w = 5.10$, $I_o = VII$ [16]) earthquakes. During the year 1783, a destructive seismic sequence started on 5 February and lasted

until 28 March (maximum Magnitude $M_w \approx 7.1$; $I_o \approx XI$ MCS [16]). The last shock of this sequence, which occurred on March 28 ($M_w = 7.03$ and $I_{max} XI$ MCS [16]) was located in the central sector of the Catanzaro Trough ([53]; see composite seismogenic source N. 9 in Figure 3B, from [35]). Although numerous seismotectonic works were undertaken in this area, the epicentral location of this shock is still debated.

On 8 September 1905, a large earthquake ($M_w = 7.5$ and MCS intensity X-XI [54]) occurred in the western sector of the Catanzaro Trough, likely offshore not far from the coastline [11,55]. This event triggered large landslides accompanied by several cracks, fractures and liquefactions, and generated a tsunami [56] with an estimated height of waves of about 2.5 m [32]. Supported by this evidence, and/or based on marine geophysical data, several authors proposed distinct source models located offshore (Figure 2B), within the Gulf of S. Eufemia [16,29,57,58]. Recently, among several minor earthquakes, two moderate seismic sequences occurred: 6 July 2017 (Maximum magnitude $M_w = 3.7$) and October 2019 (maximum magnitude $M_w = 4.0$) (Figure 2A).

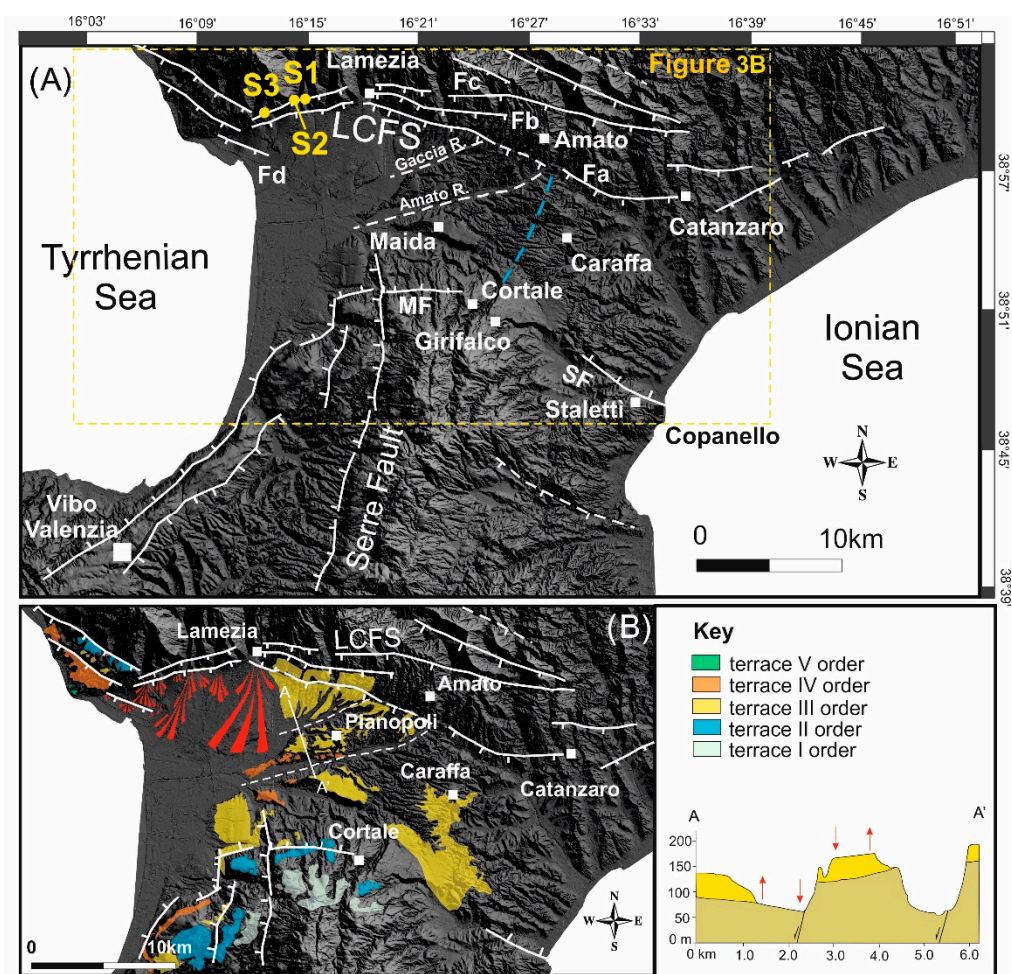


Figure 3. (A) Main faults of central-southern Calabria draped on a DEM. LCFS: Lamezia-Catanzaro Fault System, SF: Staletti Fault; MF: Maida Fault; cyan dashed line is a blind fault inferred on the basis of seismological and geodetic data (see text); yellow points are the structural stations shown in Figure 4A; (B) Detailed map showing faults (dashed where inferred), upper Pleistocene terraces and alluvial fans; the profile A-A' shows dislocated and tilted III order terrace.

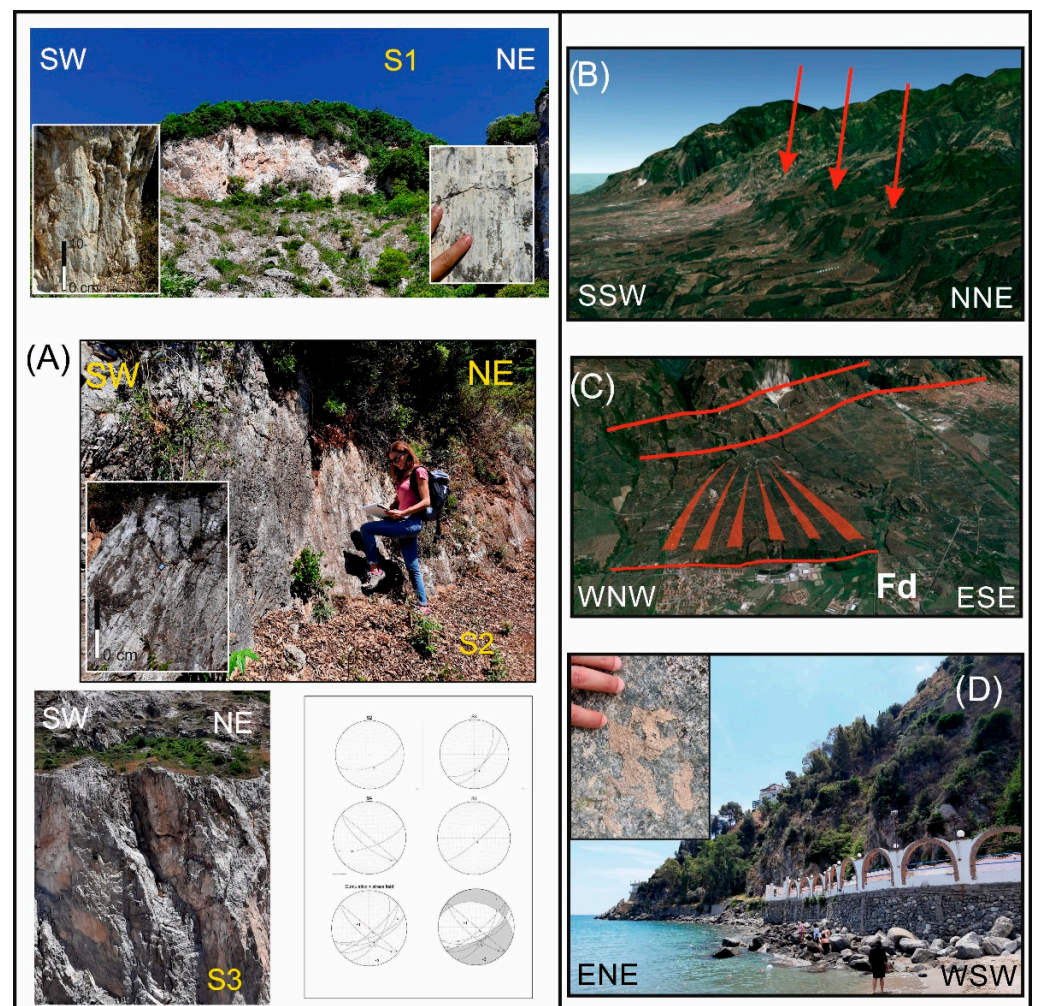


Figure 4. (A) Photos of the structural stations (see Figure 3A for location), related stereographic projections and computed stress field; (B) Trapezoidal facets created by Fa fault north of Pianopoli (see Figure 3 for location); (C) Alluvial fan dislocated by Fd fault southwest of Lamezia (see Figure 3 for location); (D) View from the south of the Staletti Fault and detail of the fault plane with evidence of slickenlines indicating oblique normal-sinistral motion.

3. Morpho-Structural Analysis

3.1. Methods

Starting from the known regional structural setting, along with the faults reported on available geological maps (Carta Geologica della Calabria, scale 1:25,000), we re-mapped the tectonic structures and analysed the surface features associated to faults. The starting point was the use of a high-resolution (5×5 m cell size) Digital Elevation Model (DEM) of the study area (Regione Calabrian, <http://geoportale.regione.calabria.it/>, accessed on 1 September 2021), managed in the GIS software platform (ArcMap 10.2 by ESRI and Global Mapper 20.1). The DEM was integrated with Lidar rendering maps to characterise the faults' geometries. Aerial stereopairs from the Italian Military Geographical Institute (1:33,000 scale) were also analysed. Finally, we performed field surveys on the major faults to check their possible recent activity and define their kinematics (Figure 4).

Structural data were collected at four key measurement stations. Fault surfaces and slickenlines were mapped and analysed using the "FieldMove[®]" software. These data were used to determine the geometry and kinematics of major faults and the principal stress orientation.

3.2. Results

The Lamezia-Catanzaro Fault System (LCFS) extends for a maximum length of ~35 km. It is composed of several 10–15 km long segments (Fa, Fb and Fc in Figure 3A) that form a set of steps in the western sector (see also [39]). The southernmost segments (Fa and Fb), which show evidence of recent activity, could be splays of the main fault (Fc) located to the north. These could have been formed when the latter became critically misaligned with the direction of maximum principal stress. Between Lamezia and the Tyrrhenian coastal area (Figure 3B), these faults displace the upper Pleistocene marine terraces and alluvial fans (conglomerate and sand deposits). Structural data collected mainly in Mesozoic limestones outcropping in the Lamezia area show a prevalence of oblique slickenlines and calcite fibres, indicating a left-lateral component of motion along the WNW–ESE striking fault planes, and prevalent normal kinematics, slightly right-lateral, along the WSW–ENE striking fault planes (Figure 4A). Morphological evidence, such as the up to 100 m high scarps with triangular and trapezoidal facets in the Pianopoli area (Figure 4B) and the displaced poly-phased alluvial fans southwest of Lamezia (Figure 4C), suggests recent normal fault activity along the WNW–ESE trending segments.

On the southeastern border of the Catanzaro Trough, a 300 m high escarpment, juxtaposing crystalline rocks with Pliocene–Middle Pleistocene deposits, characterises the WNW–ESE trending, northeast dipping, Staletti Fault (SF in Figure 3A). In particular, at the Copanello promontory along the Ionian coast (Figure 3A), the fault has displaced upper Miocene evaporitic limestones, tilted to the north. Uncertain slickenlines along the coastline suggest oblique normal–left-lateral motion (Figure 4D). Morphological and structural evidence allowed us to interpret this 6 km long structure (probably extending offshore to the east) as an exhumed fault. The W–E-trending and north-dipping Maida Fault (MF in Figure 3A) is almost 5 km long and, similarly to the Staletti Fault, shows a deeply eroded escarpment juxtaposing crystalline rocks with Pliocene–Middle Pleistocene deposits. Westwards, it is displaced by the active N–S-oriented Serre Fault (Figure 3A).

Finally, differential tilting of the middle–late Pleistocene marine terraces allowed us to infer the occurrence of two WSW–ENE trending normal faults below the Holocene deposits of the Amato and Gaccia rivers (Figure 3A). As also reported by Brutto et al. [39], these faults produced up-faulted and down-faulted blocks inside the Catanzaro Trough (see section A–A' in Figure 3B).

4. Seismological Data

4.1. Instrumental Seismicity

Seismological data (magnitude, hypocentral depth and location) of the earthquakes recorded by the INGV National Seismic Network in central Calabria in the last 40 years (see <https://istituto.ingv.it/it/risorse-e-servizi/archivi-e-banche-dati.html>, accessed on 1 September 2021) were elaborated to create a distribution map of the seismicity and relative sections in depth (Figure 5). Specifically, in order to improve the quality of the seismic dataset, the events (about 3200, with magnitude mostly in the range 1.0–3.0, with maximum magnitude 4.7) were relocated using a double-difference (DD) algorithm implemented in the tomoDDPS code [59]. The software is able to improve the locations by using a combination of absolute and differential arrival-time readings between couples of closed-spaced earthquakes, and by computing the seismic ray-tracing in a 3D velocity model; here we used the model of Scarfi et al. [25], suitable for the Calabrian area. The application of the algorithm produced a better clustering of the seismicity and a significant reduction in the residuals between the observed and theoretical arrival times of about 46%. The final locations are affected by average uncertainties of 0.35 ± 0.25 km in the epicentral coordinates and of 0.52 ± 0.35 km in depth; the average root-mean-square travel-time residual is 0.07 ± 0.03 s. The kinematics of the area (Figure 6) were analysed through the focal solutions dataset collected by Scarfi et al. [60].

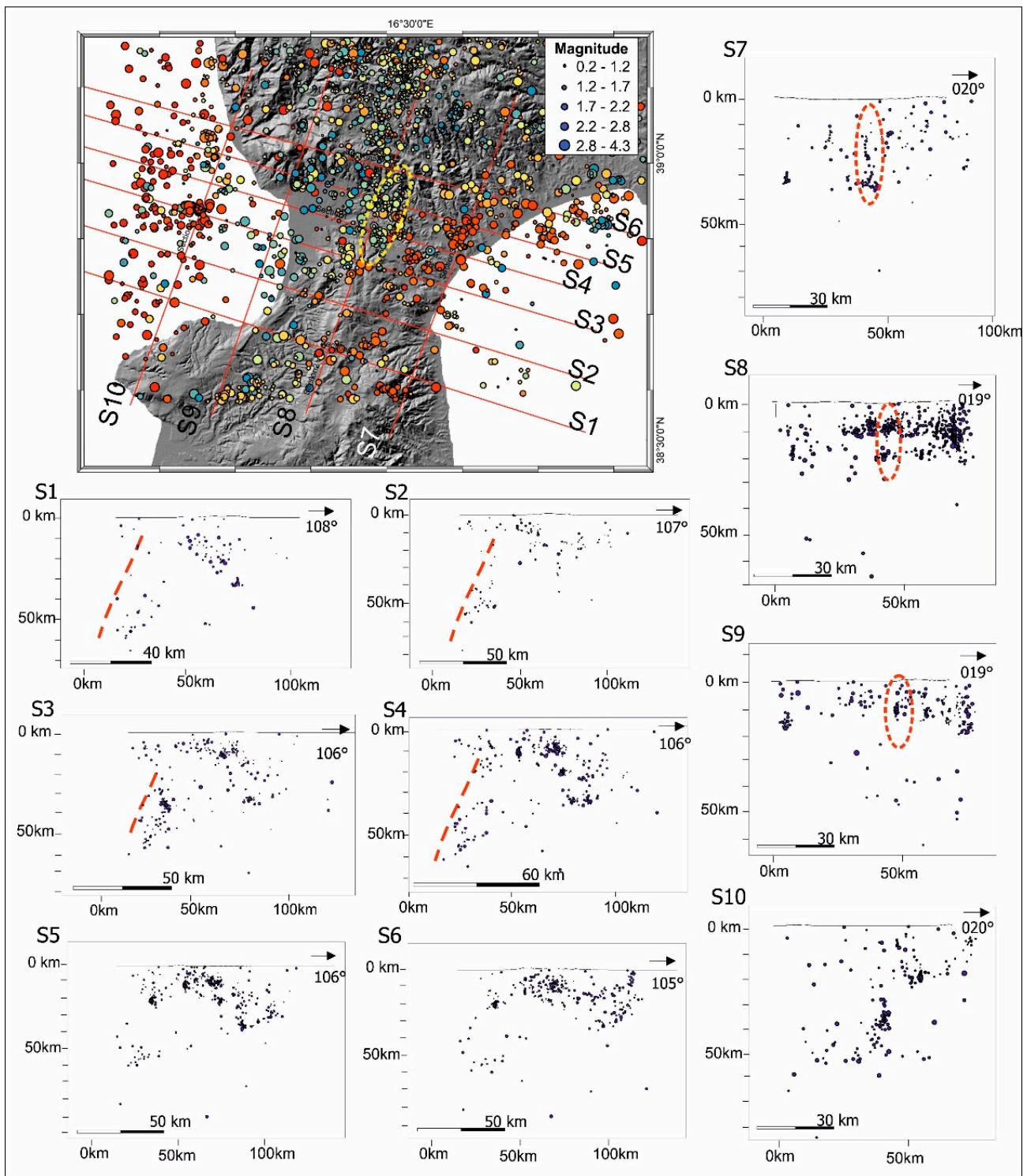


Figure 5. Map of instrumental seismicity of central Calabria and relative sections. Yellow ellipse in the map shows a roughly N–S alignment probably related to the occurrence of a blind normal fault (see text); red dashed lines in sections from s1 to s4 point out intermediate and deep earthquakes depicting the subducting Ionian slab; red ellipses in the sections from s7 to s9 make evident the high concentration of events in correspondence with the LCFS.

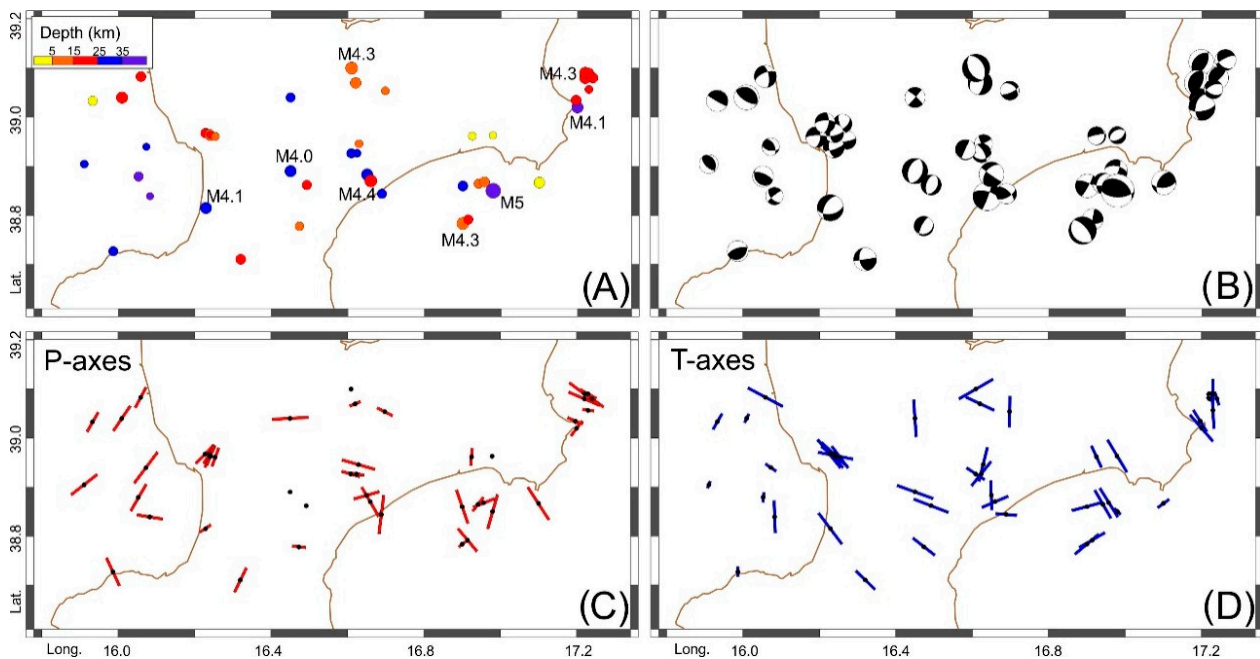


Figure 6. Earthquakes distribution available in the literature (see text); (A) Distribution in depth; (B) focal solutions; (C) P-axis distribution; (D) T-axis distribution.

4.2. Data Interpretation

The instrumental seismicity shows a high concentration of events and some clusters mainly in the northern sector of the Catanzaro Trough, in correspondence with the LCFS (see red ellipses in the sections from S7 to S9 of Figure 5), whereas diffuse seismicity characterises the southern sector. To the west, the subducting slab is well depicted by intermediate and deep earthquakes (see red line in the sections from S1 to S4 of Figure 5). In the central sector of the studied area, crustal earthquakes between 10 and 30 km of depth define a roughly N–S alignment (see yellow ellipse in the map of Figure 5).

Among the strongest recorded earthquakes, some are located close to the northern bounding fault system of the Catanzaro Trough: the 15 October 2010 event ($M_w = 4.3$) occurred about 4 kilometres from the Catanzaro city (Figure 2A); the 6 February 2015 earthquake ($M_L = 3.2$) and the 30 May 2015 event ($M_L = 3.2$) were located a few kilometres from the Cortale village (Figure 2A). In addition, the mainshock of the seismic sequence that occurred on the 6 July 2017 ($M_w = 3.7$) was located in the Ionian offshore, close to the Catanzaro coast (Figure 2A).

Focal solutions indicate prevalent left-lateral strike-slip kinematics along the WNW–ESE to ENE–WSW planes of the LCFS, whereas primarily extension on the NNE–SSW to NE–SW fault planes characterises the southwestern and central sectors of the Catanzaro Trough (Figure 6B). Additionally, it is worth noting that the focal solution of the mainshock of the seismic sequence that recently occurred in this area (7 October 2019; $M_w = 4.0$) indicates normal kinematics on the NNE–SSW fault planes, some kilometres north of the Caraffa village (Figure 2A).

The P-axis map confirms the change in the direction of the maximum stress axis, from predominantly horizontal in the northern margin of the Catanzaro Trough, along the LCFS, to vertical in the central area (Figure 6C). The T-axis map (Figure 6D) shows a predominance of the WNW–ESE oriented extension in the central area of the Catanzaro Trough.

5. Geodetic Data

5.1. IGM95-NET GNSS Monitoring

Since 1992 the Italian Istituto Geografico Militare (IGM) (<https://www.igmi.org/it/Home>, accessed on 1 September 2021) installed a new geodetic network, currently consist-

ing of 2000 benchmarks distributed throughout the Italian territory with an interdistance of about 20 km. This network has also been recently used for scientific purposes in order to calculate the coseismic deformations after the earthquakes of Colfiorito in 1997 [61] and Emilia in 2012 [62], and to estimate the active compression on southwestern Sicily [63] and in eastern Sicily [64].

We have re-surveyed six benchmarks in the Catanzaro Trough area, named as TSGI, CICA, FILA, SQUI, PZCL and SSBR, belonging to the IGM95 network (Figure 7). The benchmarks CICA and SQUI had already been surveyed three times by the IGM; TSGI, PZCL, SSBR were surveyed two times and FILA one time. In 1995, the instruments used by the IGM were Trimble 4000 SSE receivers and Trimble compact with ground plane (model 22020-00) antennas (Sunnyvale, CA, USA); during the campaigns carried out through the 2000's the instruments used by the IGM were Leica SR 530 and LEIAT 502 antenna (Wetzlar and Mannheim, Germany). The benchmarks have an average of 4.5 h of daily observation carried out by the IGM. Our occupation time is about 10 h, using Topcon HiPer SR and Topcon HiPer V receivers (L1/L2 double frequency) (Fukushima, Japan).

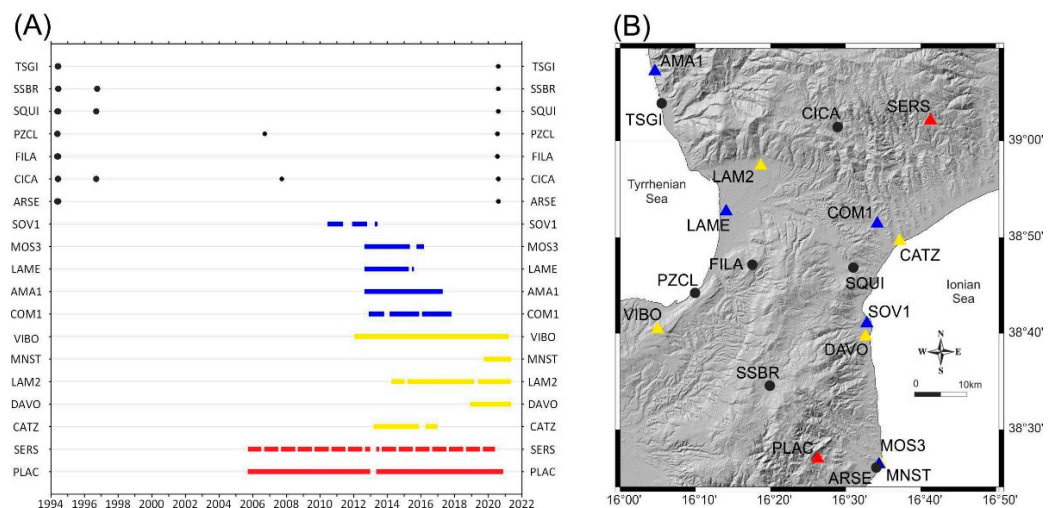


Figure 7. (A) Occupations of the benchmarks belonging to the IGM95 Network (black dots); permanent stations computed by the Nevada Geodetic Laboratory (<http://geodesy.unr.edu>, accessed on 1 September 2021) are in blue rectangles; the stations belonging to the TopNET Live (<https://www.topnetlive.com>, accessed on 1 September 2021) and RING/RDN networks are represented by yellow and red rectangles, respectively; (B) Distribution of the GNSS stations (the colours indicate the networks).

To improve the robustness of the network, we added the data of the continuous GNSS station SERS and PLAC, belonging to the RING Network (<http://ring.gm.ingv.it/>, accessed on 1 September 2021), the data of VIBO, LAM2, CATZ, CTN2, DAVO and MNST belonging to the TopNET live Italy Network (<https://rtk.topnetlive.com/italy/networks/topnet-live-italy>, accessed on 1 September 2021) and the processing of the Nevada Geodetic Laboratory (<http://geodesy.unr.edu>, accessed on 1 September 2021) of AMA1, COM1, LAME, MOS3 and SOV1 (Figure 7). The GNSS data were processed by GipsyX-1.5 [65] using precise ephemerides and clock correction provided by the Jet Propulsion Laboratory (<https://sideshow.jpl.nasa.gov>, accessed on 1 September 2021). The Earth orientation parameters are from the International Earth Rotation Services (<https://www.iers.org>, accessed on 1 September 2021). The absolute IGS antenna phase center (GPS week 1958) and the Global Mapping Function (GMF) atmospheric zenith delay models [66] were used to process data. The RINEX (Receiver INdependent EXchange) files were processed in order to estimate the position of the GNSS stations by the gd2e.py module of GipsyX, which operate in PPP (Precise Point Positioning) mode. For each Day Of the Year (DOY) we obtained covariance matrices that were used to compute the time series tied to the ITRF2014 reference frame [67].

Finally, to show adequately the current deformation field involving the Catanzaro Trough, we subtracted the velocity of eastern Sicily calculated by Carnemolla [68] to the ITRF2014 velocity of the stations. To verify the consistency of the data, we compared our results with those obtained by Palano et al. [69]. They analysed GNSS data from continuous survey stations in south Italy for a period spanning 1994–2011, aligning the horizontal GPS velocity field with respect to a fixed Hyblean-Malta block. We found an average difference of about 0.5–0.8 mm/yr between their and our velocities. Figure 8A shows the horizontal velocities of GNSS stations for the study region, with respect to the Hyblean plateau [69].

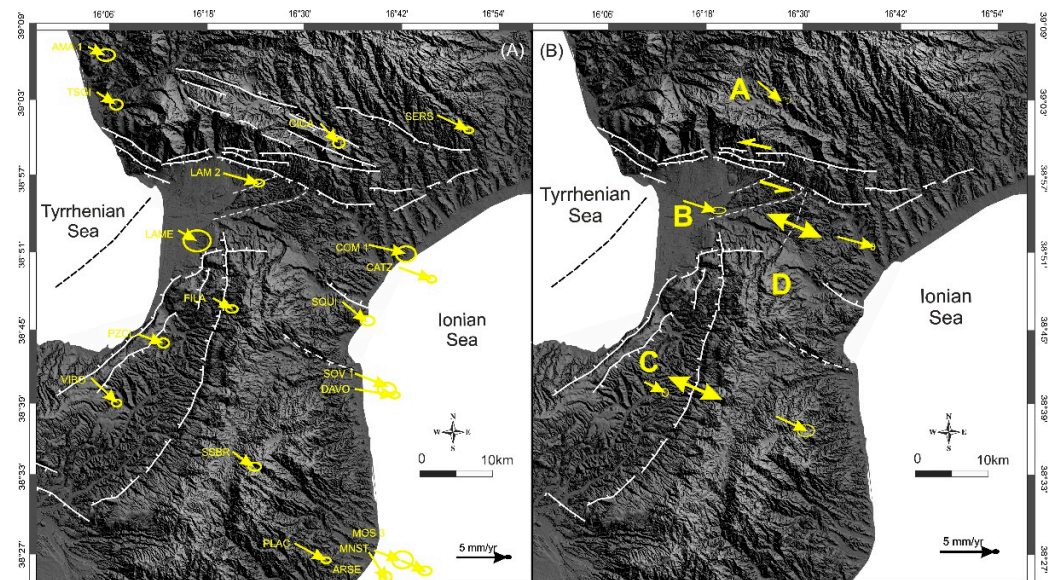


Figure 8. (A) Velocity field map of Catanzaro Trough. Velocities are referred to the Hyblean plateau [68]; (B) Velocity field map of the structural blocks and kinematics of the shear zones separating them.

5.2. Data Interpretation

Considering the tectonic frame, we divided the studied area into four blocks (A, B, C and D) in order to define the kinematics of the major fault zones (Figure 8B). The GNSS stations located inside each block were grouped in order to calculate the average velocity of each block. This was computed by the weighted average of the velocity of the stations according to their distance to the first- and second-order of regional structures and/or by taking into account if they are located inside a main active transition shear zone (Figure 8B). After that, we computed the relative velocity of each crustal block with respect to the others, to estimate the kinematics of the main shear zone (Table 1).

Table 1. Relative horizontal velocity of each crustal block (as defined in Figure 8B) with respect to the others.

Velocity [mm/yr]	A Fixed				B Fixed				C Fixed		D Fixed	
	East	North	σ_E	σ_N	East	North	East	North	East	North	East	North
A	2.11	−1.77	0.44	0.17	/	/	−1.08	−0.76	0.17	−0.58	−0.94	−0.60
B	3.19	−1.00	0.53	0.21	1.08	0.76	/	/	1.25	0.18	0.14	0.16
C	1.94	−1.19	0.18	0.22	−0.17	0.58	−1.25	−0.18	/	/	−1.10	−0.02
D	3.05	−1.16	0.47	0.41	0.94	0.60	−0.14	−0.16	1.10	0.02	/	/

Considering the east velocity, we calculated that block A shows velocities of 1.08 and 0.94 mm/yr with respect to blocks B and D, respectively. Considering the north component, we decided to neglect the deformation along this direction due to their low value with respect to their uncertainty. This implies that the Catanzaro Trough is bounded to the north by a shear zone with a prevalent left-lateral component of motion (Figure 8B)

that well matches with the present kinematics of LCFZ (see Sections 3 and 4). Between blocks C and D, we measured an extension of about 1 mm/yr associated to the Serre fault (Figures 3A and 8B). Finally, we identified the possible prolongation of the Serre fault system in the Catanzaro Trough since a differential motion of 0.14 mm/yr in the east component between the western (block B) and eastern (block D) sectors, separated by a likely blind structure, was measured (Figures 3A and 8B for the likely location of the inferred fault).

6. Discussion

Fault mapping, field survey, morpho-structural analysis and seismological/geodetic data allowed defining of the recent kinematics of the major fault system that bounds the Catanzaro Trough. To the north, the WNW–ESE to WSW–ENE-trending, south-dipping Lamezia-Catanzaro Fault System (LCFS) shows evidence of recent normal faulting since it displaces Holocene alluvial fans and shows trapezoidal and triangular facets (see also [39]). Structural analysis suggests that the LCFS has been characterised by normal-oblique left-lateral motion along the WNW–ESE-trending fault planes and normal-oblique right-lateral motion along the WSW–ENE segments (Figure 4A). Morphotectonic features highlight that the normal component of movement has been prevalent along the WSW–ENE segments (Figure 4B,C). To the south, the Plio-Quaternary deposits are displaced by minor north-dipping normal faults, Maida Fault and Staletti Fault, whose activity seems to have run out during late Quaternary times.

The seismological data indicates activity characterised by left-lateral strike-slip kinematics on roughly west–east oriented faults, in correspondence with the LCFS (Figure 6B). Notable seismic activity, characterised by extension on the NNE–SSW oriented planes, is observed in the central area of the Catanzaro Trough (Figure 6B), along the band where the WNW–ESE extension is registered between B and D blocks, even though no fault to which the seismicity could be associated outcrops. Seismicity is almost nil in the southern side of the Catanzaro Trough, thus indicating inactivity of the southern bounding faults.

Geodetic data indicate that the crustal block located north of the Catanzaro Trough (A in Figure 8B) moves towards the southeast independently and more slowly with respect to the southern block (B in Figure 8B), and such movement occurs along a belt coinciding with the LCFS; such results confirm the current left-lateral component of movement of this system. Conversely, no relative lateral movement is observed along the faults that bound the Catanzaro Trough to the south. South of the Catanzaro Trough, the WNW–ESE oriented extension is currently accommodated by the N–S oriented Serre Fault (between blocks C and D in Figure 8B). It is worth noting that the WNW–ESE oriented extension also occurs inside the Catanzaro Trough along a band separating the blocks B and D (Figure 8B), indicating the possibility of a prosecution towards the north of the extension accommodated by the Serre Fault.

Our study confirms that the Plio-Quaternary Catanzaro Trough developed as a poliphased semi-graben (see also [39]) by the activity of the major normal-oblique LCFS that bounds the basin to the north and is still controlling its development. The Maida fault and Staletti fault that bound the basin to the south appear to be minor faults, no longer active during the Holocene. It is of note that, despite structural and morphological data suggesting a late Quaternary reactivation of the LCFS according to predominantly normal kinematics (see also [2,10,39]), our geodetic and seismological data seem to indicate a current activity characterised by slight left-lateral motion. This is also confirmed by recent faulting in the S. Eufemia Gulf [51].

Considering the current kinematics, the LCFS seems to favour contemporary crustal lateral movements and local extension. Unlike the longitudinal basins of the CA (such as the Mesima and the Crati basins), which are the result of orogenic extension related to isostatic readjustment [8,40], the LCFS could be the upper crustal expression of tear-faulting related to the detachment of the northern boundary of the subducting Ionian slab (see also [52]). According to recent seismological data [25], this slab termination

seems to break progressively northwards, parallel to the trench, before being transversally detached (Figure 9). Moreover, differently from the southern boundary formed by a well-defined STEP fault system [24–26,70–72], the northern boundary of the subducting Ionian slab is interpreted as a lateral ramp that acts as a gradual transition from subduction in the Calabrian Arc to collision in the Southern Apennines (see also [24,73,74]). Thus, the LCFS transtensional belt should accommodate the lithospheric tear allowing the SE-ward advancement of the CA in the overriding plate (Figure 9). This strike-slip belt seems to extend westwards in the offshore area of the St. Eufemia Gulf where morphometric and marine geophysical data show recent fault activity [51].

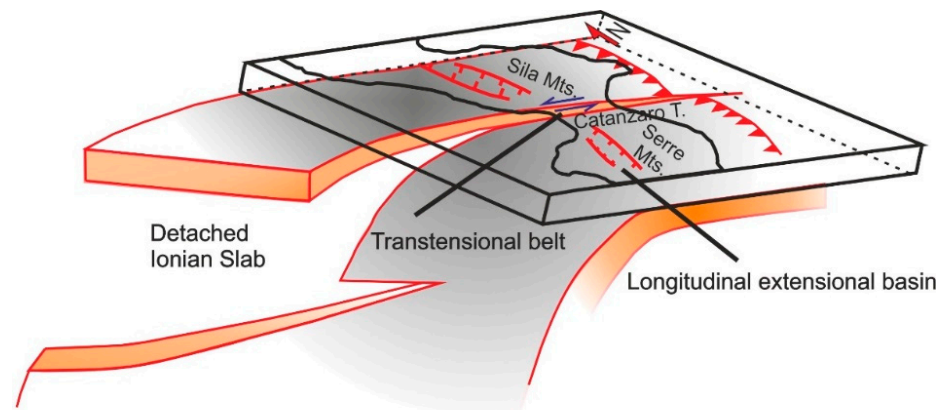


Figure 9. Geodynamic interpretation of the studied area. Detached Ionian slab depicted on the base of seismological data from Scarfi et al. [25].

As a final characterisation of the investigated active faults, we applied fault scaling relationships using fault length and kinematics to estimate the maximum expected magnitude [75,76]. For this purpose, we considered that the LCFS extends for a maximum length of ~35 km and it is composed of several 10–15 km long segments (see Section 3.2). Results indicate that the LCFS has a suitable geometrical dimension to generate earthquakes with M_w from 6 to 6.9. The epicentres of 1609, 1626, 1761 and 1821 earthquakes (magnitude between 5.10 and 6.07 [16]) are located in the northern sector of the Catanzaro Trough, at the hanging wall of LCFS (Figure 2A). Similarly, high instrumental seismic activity is observed in correspondence with the LCFS. Thus, considering the magnitude associated with both historical and instrumental earthquakes that occurred in the study area (see Section 2.2), we confirm that the LCFS could represent a possible candidate for the strong seismicity of the Catanzaro Trough region. This fault system well matches with the composite seismogenic source proposed by the DISS Working Group [35], named “Caraffa-Squillace Gulf” (Figure 2B). As regards the seismic event of 28 March 1783 ($M_w = 7.03$ and $I_{max} XI$ MCS [16]), its macroseismic epicentre should be located southwards in the central–eastern sector of the Catanzaro Trough (Figure 2A), making it difficult to attribute this event to the LCFS. However, the location of this event based on macroseismic intensity distribution could be mistaken since it occurred at the end of a disastrous seismic sequence that lasted many months and caused diffuse destruction in southern Calabria. Anyway, our seismological and geodetic data show the likely occurrence of a blind ~N–S trending seismogenic source in the central–eastern sector of the Catanzaro Trough (see yellow ellipse of the map in Figure 5), responsible for WNW–ESE extension and intermediate earthquakes.

7. Conclusions

Our multidisciplinary work, which integrates structural, geodetic and seismological data acquired in the Catanzaro Trough, allows us to draw some conclusions helpful in defining the current geodynamics of the Calabrian Arc:

- The Catanzaro Trough is a semi-graben, developed mainly by the poliphased activity of the LCFS that bounds the basin to the north. The southern faults (i.e., Maida

- and Stalettì faults) are minor, no longer active, structures that contributed to the crustal deformation.
- Geodetic and seismological data reveal that the LCFS and associated structures currently accommodate lateral crustal movements and local extension favouring the SE-ward advancement of the southern sector of the Calabrian Arc.
 - The LCFS could represent the upper crustal expression of the deep tear-faulting occurring at the northern limit of the transversally detached Ionian slab where the deep transition from subduction to collisional domain occurs.
 - Given the distribution and the magnitude of both instrumental and historical earthquakes that occurred in the Catanzaro Trough, the LCFS is responsible for the seismicity of this region. Considering its geometry and kinematics, the LCFS is capable of generating earthquakes with a magnitude up to 7.1.
 - The geodetic and seismological data highlight the occurrence of the WNW–ESE oriented extension inside the Catanzaro Trough, allowing the inference of the presence of a NNE–SSW oriented blind fault (northern prosecution of the Serre Fault) that concur with the present seismicity of the area and could have been responsible for historical events. Future research could highlight the field evidence of this inferred structure by performing paleo-seismological investigations through trench excavation.

Author Contributions: C.P. and C.M.: Conceptualization, Investigation, Methodology, Writing—original draft, Writing—review and editing, Data curation, Supervision. G.B. (Graziella Barberi), F.C., G.D.G. and L.S.: Investigation, Formal analysis, Methodology, Data curation, Visualization. G.B. (Giovanni Barreca), F.B. and F.P.: Investigation, Formal analysis, Methodology, Visualization. All authors have read and agreed to the published version of the manuscript.

Funding: This research was funded by the MUSE 4D project—Overtime tectonic, dynamic and rheologic control on destructive multiple seismic events—Special Italian Faults & Earthquakes: from real 4D cases to models in the frame of PRIN 201, grant number “2017KT2MKE”. Printing was financed by “Fondi di ateneo 2020-2022, Università di Catania, linea Open Access”.

Institutional Review Board Statement: Not applicable.

Informed Consent Statement: Not applicable.

Data Availability Statement: See text for links to publicly archived datasets analysed. Data supporting reported results are available on request by email to the corresponding author (cmonaco@unict.it).

Acknowledgments: The authors acknowledge the Direzione Geodetica of the Istituto Geografico Militare (Via di Novoli, 93—50127 Firenze) for providing data on benchmarks in the Catanzaro Trough area, belonging to the IGM95 network. The authors also acknowledge the use of MOVE Software Suite granted by Petroleum Experts Limited (www.petex.com, accessed on 1 September 2021).

Conflicts of Interest: The authors declare no conflict of interest.

References

1. Malinverno, A.; Ryan, W.B.F. Extension in the Tyrrhenian sea and shortening in the Apennines as result of arc migration driven by sinking of the lithosphere. *Tectonics* **1986**, *5*, 227–245. [[CrossRef](#)]
2. Tansi, C.; Muto, F.; Critelli, S.; Iovine, G. Neogene-Quaternary strike-slip tectonics in the central Calabria Arc (southern Italy). *J. Geodyn.* **2007**, *43*, 397–414. [[CrossRef](#)]
3. Faccenna, C.; Becker, T.W.; Lucente, F.P.; Jolivet, L.; Rossetti, F. History of subduction and back arc extension in the Central Mediterranean. *Geophys. J. Int.* **2001**, *145*, 809–820. [[CrossRef](#)]
4. Faccenna, C.; Funicello, F.; Civetta, L.; D’Antonio, M.; Moroni, M.; Piroallo, C. Slab disruption, mantle circulation, and the opening of the Tyrrhenian basins. *Geol. Soc. Am. Spec. Pap.* **2007**, *418*, 153–169. [[CrossRef](#)]
5. Neri, G.; Barberi, G.; Oliva, G.; Orecchio, B. Spatial variations of seismogenic stress orientations in Sicily, south Italy. *Phys. Earth and Planet. Int.* **2005**, *148*, 175–191. [[CrossRef](#)]
6. D’Agostino, N.; D’Anastasio, E.; Gervasi, A.; Guerra, I.; Nedimović, M.R.; Seeber, L.; Steckler, M. Forearc extension and slow rollback of the Calabrian Arc from GPS measurements. *Geophys. Res. Lett.* **2011**, *38*, L17304. [[CrossRef](#)]
7. Presti, D.; Billi, A.; Orecchio, B.; Totaro, C.; Faccenna, C.; Neri, G. Earthquake focal mechanisms, seismogenic stress, and seismotectonics of the Calabrian Arc, Italy. *Tectonophysics* **2013**, *602*, 153–175. [[CrossRef](#)]

8. Ghisetti, F.; Vezzani, L. Different styles of deformation in the Calabrian arc (southern Italy): Implications for a seismotectonic zoning. *Tectonophysics* **1982**, *85*, 149–165. [[CrossRef](#)]
9. Tortorici, L.; Monaco, C.; Tansi, C.; Cocina, O. Recent and active tectonics in the Calabrian Arc (Southern Italy). *Tectonophysics* **1995**, *243*, 37–55. [[CrossRef](#)]
10. Monaco, C.; Tortorici, L. Active faulting in the Calabrian arc and eastern Sicily. *J. Geod.* **2000**, *29*, 407–424. [[CrossRef](#)]
11. Gasparini, C.; Iannaccone, G.; Scandone, P.; Scarpa, R. Seismotectonics of the Calabrian Arc. *Tectonophysics* **1982**, *82*, 267–286. [[CrossRef](#)]
12. Westaway, R. Seismic moment summation for historical earthquakes in Italy: Tectonic implications. *J. Geophys. Res.* **1992**, *97*, 15437–15464. [[CrossRef](#)]
13. Castello, B.; Selvaggi, G.; Chiarabba, C.; Amato, A. *CSI Catalogo della Sismicità Italiana 1981–2002, Versione 1.1.*; INGV-CNT: Rome, Italy, 2006. Available online: <http://csi.rm.ingv.it/> (accessed on 1 September 2021).
14. Calò, M.; Dorbath, C.; Luzio, D.; Rotolo, S.G.; D’Anna, G. Seismic velocity structures of southern Italy from tomographic imaging of the Ionian slab and petrological inferences. *Geophys. J. Int.* **2012**, *191*, 751–764. [[CrossRef](#)]
15. Rotondi, R. Bayesian nonparametric inference for earthquake recurrence time distributions in different tectonic regimes. *J. Geophys. Res. Solid Earth* **2010**, *115*, B01302. [[CrossRef](#)]
16. Rovida, A.; Locati, M.; Camassi, R.; Lolli, B.; Gasperini, P.; Antonucci, A. *Italian Parametric Earthquake Catalogue (CPTI15), Version 3.0.*; Istituto Nazionale di Geofisica e Vulcanologia (INGV): Rome, Italy, 2021. [[CrossRef](#)]
17. Van Dijk, J.P.; Bello, M.; Brancaleoni, G.P.; Cantarella, G.; Costa, V.; Frixia, A.; Golfetto, F.; Merlini, S.; Riva, M.; Torricelli, S.; et al. A regional structural model for the northern sector of the Calabrian Arc (southern Italy). *Tectonophysics* **2000**, *324*, 267–320. [[CrossRef](#)]
18. Ghisetti, F. Evoluzione neotettonica dei principali sistemi di faglie della Calabria centrale. *Boll. Soc. Geol. Ital.* **1979**, *98*, 387–430.
19. Ghisetti, F. Upper Pliocene-Pleistocene uplift rates as indicators of neotectonic pattern: An example from southern Calabria (Italy). *Z. für Geomorphol.* **1981**, *40*, 93–118.
20. Minelli, L.; Faccenna, C. Evolution of the Calabrian accretionary wedge (central Mediterranean). *Tectonics* **2010**, *29*, TC4004. [[CrossRef](#)]
21. Sartori, R. The Tyrrhenian back-arc basin and subduction of the Ionian lithosphere. *Episodes* **2003**, *26*, 217–221. [[CrossRef](#)]
22. Patacca, F.; Sartori, R.; Scandone, P. Tyrrhenian basin and Apenninic arcs: Kinematic relations since Late Tortonian times. *Mem. Soc. Geol. Ital.* **1990**, *45*, 425–451.
23. Orecchio, B.; Presti, D.; Totaro, C.; Neri, G. What earthquakes say concerning residual subduction and STEP dynamics in the Calabrian Arc region, south Italy. *Geophys. J. Int.* **2014**, *199*, 1929–1942. [[CrossRef](#)]
24. Maesano, F.E.; Tiberti, M.M.; Basili, R. The Calabrian Arc: Three dimensional modelling of the subduction interface. *Sci. Rep.* **2017**, *7*, 8887. [[CrossRef](#)]
25. Scarfi, L.; Barberi, G.; Barreca, G.; Cannavò, F.; Koulakov, I.; Patanè, D. Slab narrowing in the Central Mediterranean: The Calabro-Ionian subduction zone as imaged by high resolution seismic tomography. *Sci. Rep.* **2018**, *8*, 5178. [[CrossRef](#)]
26. Barreca, G.; Scarfi, L.; Gross, F.; Monaco, C.; De Guidi, G. Fault Pattern and Seismotectonic Potential at the South-Western Edge of the Ionian Subduction System (Southern Italy): New Field and Geophysical Constraints. *Tectonophysics* **2019**, *761*, 31–45. [[CrossRef](#)]
27. Wortel, R.; Spakman, W. Subduction and slab detachment in the Mediterranean-Carpathian region. *Science* **2000**, *290*, 1910–1917. [[CrossRef](#)] [[PubMed](#)]
28. De Ritis, R.; Pepe, F.; Orecchio, B.; Casalbore, D.; Bosman, A.; Chiappini, M.; Chiocci, F.; Corradino, M.; Nicolich, R.; Martorelli, E.; et al. Magmatism along lateral slab-edges: Insights from the Diamante-Enotrio-Ovidio Volcanic-Intrusive Complex (Southern Tyrrhenian Sea). *Tectonics* **2019**, *38*, 2581–2605. [[CrossRef](#)]
29. Loreto, M.F.; Fracassi, U.; Franzo, A.; Del Negro, P.; Zgur, F.; Facchin, L. Approaching the potential seismogenic source of the 8 September 1905 earthquake: New geophysical, geological and biochemical data from the S. Eufemia Gulf (S Italy). *Mar. Geol.* **2013**, *343*, 62–75. [[CrossRef](#)]
30. Peruzza, L.; Pantosti, D.; Slejko, D.; Valensise, G. Testing a new hybrid approach to seismic hazard assessment: An application to the Calabrian Arc (Southern Italy). *Nat. Hazards* **1997**, *14*, 113–126. [[CrossRef](#)]
31. Valensise, G.; Pantosti, D. Seismogenic faulting, moment release patterns and seismic hazard along the central and southern Apennines and the Calabrian arc. In *Anatomy of an Orogen: The Apennines and Adjacent Mediterranean Basins*; Vai, G.B., Martini, I.P., Eds.; Kluwer Academic Publishers: Dordrecht, The Netherlands, 2001; pp. 495–512.
32. Piatanesi, A.; Tinti, S. Numerical modelling of the September 8, 1905 Calabrian (southern Italy) tsunami. *Geophys. J. Int.* **2002**, *150*, 271–284. [[CrossRef](#)]
33. Cucci, L.; Tertulliani, A. I terrazzi marini nell’area di Capo Vaticano (Arco Calabro): Solo un record di sollevamento regionale o anche di deformazione cosismica? *Il Quaternario* **2006**, *19*, 89–101.
34. Cucci, L.; Tertulliani, A. The Capo Vaticano (Calabria) coastal terraces and the 1905 M7 earthquake: The geomorphological signature of the regional uplift and coseismic slip in southern Italy. *Terra Nova* **2010**, *22*, 378–389. [[CrossRef](#)]
35. DISS Working Group. *Database of Individual Seismogenic Sources (DISS), Version 3.2.1: A Compilation of Potential Sources for Earthquakes Larger than M 5.5 in Italy and Surrounding Areas*. Istituto Nazionale di Geofisica e Vulcanologia. 2018. Available online: <http://diss.rm.ingv.it/diss/> (accessed on 1 September 2021). [[CrossRef](#)]

36. Turco, E.; Maresca, R.; Cappadona, P. Plio-Pleistocene tectonics at the Calabrian-Lucanian boundary: A kinematic model. *Mem. Soc. Geol. Ital.* **1990**, *45*, 519–529.
37. Van Dijk, J.P.; Scheepers, P.J.J. Neogene rotations in the Calabrian Arc. Implications for a Pliocene-Recent geodynamic scenario for the central Mediterranean. *Earth Sci. Rev.* **1995**, *39*, 207–246. [[CrossRef](#)]
38. Del Ben, A.; Barnaba, C.; Taboga, A. Strike-slip systems as the main tectonic features in the Plio-Quaternary kinematics of the Calabrian Arc. *Mar. Geophys. Res.* **2008**, *29*, 1–12. [[CrossRef](#)]
39. Brutto, F.; Muto, F.; Loreto, M.F.; De Paola, N.; Tripodi, V.; Critelli, S.; Facchin, L. The Neogene-Quaternary geodynamic evolution of the central Calabrian Arc: A case study from the western Catanzaro Trough basin. *J. Geodyn.* **2016**, *102*, 95–114. [[CrossRef](#)]
40. Westaway, R. Quaternary uplift of southern Italy. *J. Geophys. Res.* **1993**, *98*, 21741–21772. [[CrossRef](#)]
41. Doglioni, C.; Innocenti, F.; Mariotti, G. Why Mt. Etna? *Terra Nova* **2001**, *13*, 25–31. [[CrossRef](#)]
42. Miyauchi, T.; Dai Pra, G.; Labini, S.S. Geochronology of Pleistocene marine terraces and regional tectonics in the Tyrrhenian coast of south Calabria, Italy. *Il Quaternario* **1994**, *7*, 17–34.
43. Bianca, M.; Catalano, S.; De Guidi, G.; Gueli, A.M.; Monaco, C.; Ristuccia, G.M.; Stella, G.; Tortorici, G.; Tortorici, L.; Troja, S.O. Luminescence chronology of Pleistocene marine terraces of Capo Vaticano Peninsula (Calabria, Southern Italy). *Quatern. Int.* **2011**, *232*, 114–121. [[CrossRef](#)]
44. Ferranti, L.; Antonioli, F.; Mauz, B.; Amorosi, A.; Dai Pra, G.; Mastronuzzi, G.; Monaco, C.; Orrù, P.; Pappalardo, M.; Radtke, U.; et al. Markers of the last interglacial sea-level high stand along the coast of Italy: Tectonic implications. *Quatern. Int.* **2006**, *14*, 30–54. [[CrossRef](#)]
45. Monaco, C.; Barreca, G.; Di Stefano, A. Quaternary marine terraces and fault activity in the northern mainland sectors of the Messina Straits (southern Italy). *Ital. J. Geosci.* **2017**, *136*, 337–346. [[CrossRef](#)]
46. Pepe, F.; Bertotti, G.; Ferranti, L.; Sacchi, M.; Collura, A.M.; Passaro, S.; Sulli, A. Pattern and rate of post-20 ka vertical tectonic motion around the Capo Vaticano Promontory (W Calabria, Italy) based on offshore geomorphological indicators. *Quatern. Int.* **2014**, *332*, 85–98. [[CrossRef](#)]
47. Ferrini, G.; Testa, G. La successione miocenica superiore della Stretta di Catanzaro, dati preliminari. In Proceedings of the Abstracts of the Gruppo di Sedimentologia del CNR, Annual Meeting, 474, Arcavacata di Rende, Italy, 13–17 October 1997; pp. 53–55.
48. Cavazza, W.; Decelles, P.G. Upper Messinian siliciclastic rocks in southeastern Calabria (S Italy): Paleotectonic and eustatic implications for the evolution of the central Mediterranean region. *Tectonophysics* **1998**, *298*, 223–241. [[CrossRef](#)]
49. Longhitano, S.G.; Chiarella, D.; Muto, F. Three-dimensional to two-dimensional cross-strata transition in the lower Pleistocene Catanzaro tidal strait transgressive succession (southern Italy). *Sedimentology* **2014**, *61*, 2136–2171. [[CrossRef](#)]
50. Punzo, M.; Cianflone, G.; Cavuoto, G.; De Rosa, R.; Dominici, R.; Gallo, P.; Lirer, F.; Pelosi, N.; Di Fiore, V. Active and passive seismic methods to explore areas of active faulting. The case of Lamezia Terme (Calabria, southern Italy). *J. Appl. Geophys.* **2021**, *188*, 104316. [[CrossRef](#)]
51. Corradino, M.; Pepe, F.; Burrato, P.; Kanari, M.; Parrino, N.; Bertotti, G.; Bosman, A.; Casalbore, D.; Ferranti, L.; Martorelli, E.; et al. An integrated multiscale method for the characterization of active faults in offshore areas. The case of Sant’Eufemia Gulf (Offshore Calabria, Italy). *Front. Earth Sci.* **2021**, *9*, 670557. [[CrossRef](#)]
52. Guarnieri, P. Plio-Quaternary segmentation of the south Tyrrhenian forearc basin. *Int. J. Earth Sci.* **2006**, *95*, 107–118. [[CrossRef](#)]
53. Jacques, E.; Monaco, C.; Tapponnier, P.; Tortorici, L.; Winter, T. Faulting and earthquake triggering during the 1783 Calabria seismic sequence. *Geophys. J. Int.* **2001**, *147*, 499–516. [[CrossRef](#)]
54. Michelini, A.; Lomax, A.; Nardi, A.; Rossi, A. La localizzazione del terremoto della Calabria dell’8 settembre 1905 da dati strumentali. In *8 Settembre 1905, Terremoto in Calabria*; Guerra, I., Savaglio, A., Eds.; Università della Calabria: Calabria, Italy, 2006; pp. 225–240.
55. Boschi, E.; Guidoboni, E.; Ferrari, G.; Mariotti, D.; Valensise, G.; Gasperini, P. Catalogue of Strong Italian Earthquakes from 461 B.C. to 1997. *Ann. Geofis.* **2000**, *43*, 259.
56. Tinti, S.; Maramai, A.; Graziani, L. The New Catalogue of Italian Tsunamis. *Nat. Hazards* **2004**, *33*, 439–465. [[CrossRef](#)]
57. Riuscetti, M.; Schick, R. Earthquakes and tectonics in Southern Italy. *Boll. Geofis. Teor. Appl.* **1975**, *17*, 59–78.
58. Camassi, R.; Stucchi, M. *NT4.1.1, un Catalogo Parametrico di Terremoti di Area Italiana al di Sopra Della Soglia del Danno*; Gruppo Nazionale Difesa dai Terremoti, Rapp: Interno, Milano, 1997; p. 95.
59. Zhang, H.; Thurber, C.; Bedrosian, P. Joint inversion for Vp, Vs, and Vp/Vs at SAFOD, Parkfield, California. *Geochem. Geophys. Geosyst.* **2009**, *10*, 17. [[CrossRef](#)]
60. Scarfi, L.; Langer, H.; Messina, A.; Musumeci, C. Tectonic Regimes Inferred From Clustering of Focal Mechanisms and Their Distribution in Space: Application to the Central Mediterranean Area. *J. Geophys. Res. Solid Earth* **2020**, *125*, e2020JB020519. [[CrossRef](#)]
61. Anzidei, M.; Baldi, P.; Serpelloni, E. The coseismic ground deformations of the 1997 Umbria-Marche earthquakes: A lesson for the development of new GPS networks. *Ann. Geophys.* **2008**, *51*, 343–359.
62. Serpelloni, E.; Anderlini, L.; Avallone, A.; Cannelli, V.; Cavaliere, A.; Cheloni, D.; D’Ambrosio, C.; D’Anastasio, E.; Esposito, A.; Pietrantonio, G.; et al. GPS observations of coseismic deformation following the May 20 and 29, 2012, Emilia seismic events (northern Italy): Data, analysis and preliminary models. *Ann. Geophys.* **2012**, *55*, 759–766. [[CrossRef](#)]

63. Barreca, G.; Bruno, V.; Cocorullo, C.; Cultrera, F.; Ferranti, L.; Guglielmino, F.; Guzzetta, L.; Mattia, M.; Monaco, C.; Pepe, F. Geodetic and geological evidence of active tectonics in south-western Sicily (Italy). *J. Geodyn.* **2014**, *82*, 138–149. [[CrossRef](#)]
64. De Guidi, G.; Barberi, G.; Barreca, G.; Bruno, V.; Cultrera, F.; Grassi, S.; Imposa, S.; Mattia, M.; Monaco, C.; Scarfi, L.; et al. Geological, seismological and geodetic evidence of active thrusting and folding south of Mt. Etna (eastern Sicily): Reevaluation of “seismic efficiency” of the Sicilian Basal Thrust. *J. Geodyn.* **2015**, *90*, 32–41. [[CrossRef](#)]
65. Bertiger, W.; Bar-Sever, Y.; Dorsey, A.; Haines, B.; Harvey, N.; Hemberger, D.; Heflin, M.; Lu, W.; Miller, M.; Moore, A.W.; et al. GipsyX/RTGx, a new tool set for space geodetic operations and research. *Adv. Sp. Res.* **2020**, *66*, 469–489. [[CrossRef](#)]
66. Boehm, J.; Niell, A.; Tregoning, P.; Schuh, H. Global Mapping Function (GMF): A new empirical mapping function based on numerical weather model data. *Geophys. Res. Lett.* **2006**, *33*, L07304. [[CrossRef](#)]
67. Altamimi, Z.; Rebischung, P.; Métivier, L.; Collilieux, X. ITRF2014: A new release of the International Terrestrial Reference Frame modeling nonlinear station motions. *J. Geophys. Res. Solid Earth* **2016**, *121*, 6109–6131. [[CrossRef](#)]
68. Carnemolla, F. Monitoring and Analysis of Surface Deformation Using Comparative Geodetic and Topographic Techniques. Case Study of the Eastern Slope of the Etna Volcano. Ph.D. Thesis, University of Catania, Catania, Italy, 2021; 180p.
69. Palano, M.; Ferranti, L.; Mattia, M.; Monaco, C.; Aloisi, M.; Bruno, V.; Cannavò, F.; Siligato, G. GPS velocity and strain fields in Sicily and southern Calabria, Italy: Updated geodetic constraints on tectonic block interaction in the central Mediterranean. *J. Geophys. Res.* **2012**, *117*, B07401. [[CrossRef](#)]
70. Gutscher, M.; Dominguez, S.; Mercier de Lepinay, B.; Pinheiro, L.; Gallais, F.; Babonneau, N.; Cattaneo, A.; Le Faou, Y.; Barreca, G.; Micallef, A.; et al. Tectonic expression of an active slab tear from high-resolution seismic and bathymetric data offshore Sicily (Ionian Sea). *Tectonics* **2015**, *35*, 39–54. [[CrossRef](#)]
71. Polonia, A.; Torelli, L.; Artoni, A.; Carlini, M.; Faccenna, C.; Ferranti, L.; Gasperini, L.; Govers, R.; Klaeschen, D.; Monaco, C.; et al. The Ionian and Alfeo-Etna fault zones: New segments of an evolving plate boundary in the central Mediterranean Sea? *Tectonophysics* **2016**, *675*, 69–90. [[CrossRef](#)]
72. Maesano, F.E.; Tiberti, M.M.; Basili, R. Deformation and Fault Propagation at the Lateral Termination of a Subduction Zone: The Alfeo Fault System in the Calabrian Arc, Southern Italy. *Front. Earth Sci.* **2020**, *8*, 107. [[CrossRef](#)]
73. Neri, G.; Marotta, A.M.; Orecchio, B.; Presti, D.; Totaro, C.; Barzaghi, R.; Borghi, A. How lithospheric subduction changes along the Calabrian Arc in southern Italy: Geophysical evidences. *Int. J. Earth Sci.* **2012**, *101*, 1949–1969. [[CrossRef](#)]
74. Totaro, C.; Koulakov, I.; Orecchio, B.; Prestia, D. Detailed crustal structure in the area of the southern Apennines–Calabrian Arc border from local earthquake tomography. *J. Geodyn.* **2014**, *82*, 87–97. [[CrossRef](#)]
75. Wells, D.; Coppersmith, K. New empirical relationships among magnitude, rupture length, rupture width, rupture area, and surface displacement. *Bull. Seismol. Soc. Am.* **1994**, *84*, 974–1002.
76. Pace, B.; Visini, F.; Peruzza, L. FiSH: MATLAB tools to turn fault data into Seismic-Hazard Models. *Seism. Res. Lett.* **2016**, *87*, 374–386. [[CrossRef](#)]